

## Design guidelines for proximity coupled U-slot microstrip antennas

Marzieh Nasirian<sup>1</sup>, Zaker Hossein Firouzeh<sup>2</sup>,  
Mohsen Maddah-Ali<sup>2</sup>, Gholam Reza Askari<sup>1</sup>

Received:2016-01-20

Accepted:2016-09-02

### Abstract

The frequency bandwidth of microstrip patch antennas can be increased using both of U-slot and proximity feeding. Although some design rules have been already explained for the probe-fed U-slot antenna the proximity coupling causes to consider a lot of parameters for design procedure; consequently, to deal with all of them seems confusing. In this paper after investigating the effect of various parameters on the multiple resonant frequencies of the antenna and recognizing the most effective factors, some guidelines to design a proximity coupled U-slot microstrip antenna are proposed. In addition, an antenna element with 16% impedance bandwidth is designed at center frequency of 16.7GHz, and its broadband impedance and radiation characteristics are vastly considered. Also, 1×2 and 2×2 arrays of the antenna element are designed to use as subarrays for designing large arrays. The measurement results of return loss and radiation pattern, show good agreement with simulation results.

**Keywords—** microstrip antenna; U-slot; proximity coupled feed; wide band

### I. INTRODUCTION

Microstrip antennas are widely used because of their low profile, light weight, low cost and their ability to form large and conformal arrays. However, often the main drawback of microstrip antennas used in wideband communication systems is their narrow bandwidth. So far, lots of methods have been introduced to remedy this problem. These bandwidth broadening techniques are mainly based on two approaches [1]; one is to

add a matching component to the structure like matching stubs in the microstrip antenna feed-line, and the other one is to increase the number of resonating elements with close resonant frequencies like parasitic elements or slots in the radiating patch. Unfortunately, structures like stacked and parasitic patches considerably increase the whole profile of the antenna. Besides these techniques, some feeding methods like aperture-coupling and proximity-coupling were proposed to broaden the antenna bandwidth. Meanwhile, other antenna parameters such as return loss, gain and beamwidth should be noted and optimized.

It is observed that a simple rectangular slot in the patch causes a narrower pass-band,[2] but a U-shaped slot, firstly used by Huynh and Lee in 1995, can efficiently improve the antenna bandwidth by increasing the number of antenna resonant frequencies.[3] Since then, the probe-fed U-slot microstrip antenna has been widely used, not only for broadband designs, but also for multi-band and band notch operations and circular polarization applications.[4] Besides the main advantage of improving the bandwidth, the U-slot causes a little increment in antenna gain. On the other hand, the X-pol level increases and the antenna main beam is a little turned due to the asymmetry in the structure.

Moreover, some broadband techniques have been combined to develop more interesting methods. For example, a U-shaped slot in the patch with proximity coupled feed, in which a  $\Pi$ -shaped stub was used in the feed-line, was advised in 1998.[5] This stub makes a proper coupling between the feed and patch and it prepares a matching circuit, as well. In another work, the matching impedance was not degraded regarding to lateral displacement of the feed using two stubs, however, the cross polarization level was increased.[6] In 2002, Kidder et al. changed the stubs to a double  $\Pi$ -shaped feed line and implemented the feed stubs completely beneath the patch to achieve a compact array antenna.[7] This approach was used in [8] to design a large array in Ku-band frequencies for SAR applications.

In [9-11], some studies have been done to analyze the single layer U-slot microstrip antenna. Also, the frequency behavior of the antenna which is dependent on antenna dimensions such as the patch dimensions and the length of U-slot arms has been investigated in [12-14]. Using proximity coupling method instead of probe feeding, causes

<sup>1</sup> MSc., Electrical engineering, communication - Field and wave Dept. of Electrical and Computer Engineering Isfahan University of Technology (IUT).Email: m.nasirian@ec.iut.ac.ir

Email: askarigh@ec.iut.ac.ir

<sup>2</sup> PhD., Electrical engineering, communication - Field and wave Assistant professor, Dept. of Electrical and Computer Engineering ,Isfahan University of Technology (IUT)

Email: zhfirouzeh@ec.iut.ac.ir, Email: maddahali@ec.iut.ac.ir

a lot of new parameters to be considered in the design procedure, and the influence and importance of each parameter to be investigated. As a result, some practical guidelines should be used to design a wideband antenna.

In this paper, the proximity coupled-fed method to design U-Slot microstrip array antenna is extensively studied. After description of the antenna structure, which is based on the geometry introduced in [8], in Section 2, a parametric study is explained and the influence of main parameters on the antenna characteristics is considered in Section 3. Then, a design procedure is reviewed and some design guidelines are proposed in Section 4. Finally, a single-element antenna and 1×2 and 2×2 array antennas are designed, simulated and fabricated. It is illustrated that the simulation and measurement results are in good agreement.

II. ANTENNA STRUCTURE

The proximity coupled-fed antenna with a two-layer structure is shown in Figure 1. The feed network \_a Π-shaped feed with an additional stub\_ is embedded between two substrates, and through electromagnetic coupling excites the U-slot patch printed on the top of the upper substrate (the top view is presented in Figure 2). The bottom of the lower substrate is used as the metal ground. The feed stubs are designed so that they extend up to under the patch edges. As mentioned before, the Π-shaped feed prepares a good coupling between the feed and U-shaped slot ,and so provides wideband characteristics. In case of

simple Π feed, the antenna main beam turns a little toward the U-slot opening, however adding the additional upper stub to the feed, nearly compensates this rotation; this stub also has some effects on increasing antenna gain and reducing the electrical size of the antenna element. In order to reduce the undesirable radiation from the feed lines, the thickness of the lower substrate is less than the upper one.[15] Duroid 5880 with 20 and 31-mil thickness as the lower and upper substrates, respectively, are used to fabricate the antenna.

III. PARAMETRIC STUDIES

The first step of antenna design is to specify input impedance, and to ensure a good impedance matching over the desired frequency band.[16] So, in order to find the frequency dependent behaviour of the antenna, the return loss or reflection coefficient diagram is examined. The return loss of the proposed antenna consists of two resonances; one for U-slot in the patch, and another one for the patch itself. Figure 2 is the top view of the antenna which shows the patch, U-slot, and feed-lines along with all dimensional parameters simultaneously. To provide design guidelines, the effects of these parameters on the frequency behavior of the antenna are investigated through the parametric study. Initial dimensions depicted in Table 1 are obtained from the design procedure presented in the following section. In the parametric study only one parameter is investigated at a time while all other parameters are kept fixed.

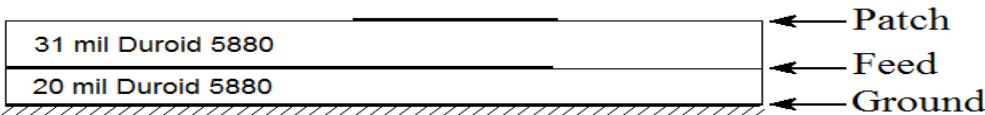


Figure 1. Geometrv of the proximity coupled-fed microstrip antenna.

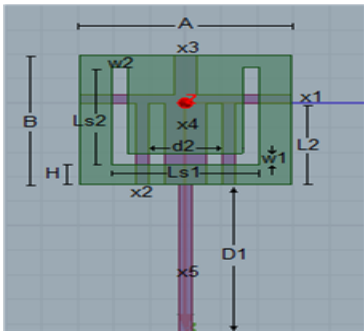


Figure 2. The top view of the proximity coupled-fed antenna.

Table 1. Initial dimensions.

Name	Value	Unit
w1	0.45	mm
w2	0.45	mm
Ls1	4.11	mm
Ls2	3.51	mm
L2	3.33	mm
d2	2.03	mm
x1	0.36	mm
x2	0.36	mm
x3	0.61	mm
x4	1.2	mm
x5	0.36	mm
B	5.3	mm
H	0.82	mm
A	5.92	mm

### A. Parametric Results

The parametric study results are summarized in Table 2. This table represents qualitative relationships between different dimensions and antenna properties. There, "f1" and "f2" are the first and second resonant frequencies, respectively, and "fc" stands for the central frequency of -10dB bandwidth. Also, "return loss (RL) level", represents the value of return loss corresponding to the local maximum value of S11(dB) within the pass-band. Note that the return loss is negative of the input reflection coefficient. For example, the table indicates that increasing the patch width (A+), decreases both of the resonant frequencies, but affects the second one dramatically (indicated by "-" and "--", respectively). It also increases the RL level leading to a better impedance matching. A zero ("0") in the table means that the influence of the parameter can be neglected. While in the case of "0(-)" or "0(+)", the change is a little more considerable, but it is still insignificant.

### B. Discussion

As noted in Table 2, the frequency behavior of the antenna is significantly dependent on these parameters: the patch length (B) and width (A), the length of the downward vertical feed stubs (L2), and the length of U-slot arms (Ls2). As expected, the frequency behavior of the antenna is significantly dominated by the patch length (B) which is about 0.44 of the guided wavelength in substrate (the patch width (A) is a little more (0.49 of the guided wavelength)). The parametric study of the main parameters including A, B, L2,

and Ls2 are illustrated in Figure 4. The other parameters have less influence such as the horizontal distance between the two downward feed stubs (d2), the U-slot offset from the patch edge (H), the U-slot base length (Ls1) and also, the width of some feed-line parts, namely x2, x4 and x5. The effectiveness of the slot widths (w1 and w2), and the width of other parts of feed (x1 and x3) are negligible. Some further results and observations are listed below:

- As expected, the first resonance is dominantly determined by the patch length (B) corresponding to the patch resonance.
- The second resonant frequency is affected by the patch width (A), L2 and Ls2. Also, B, d2 and x2 but it is less dominant. Therefore, this frequency strongly depends on the U-slot resonance, since Ls2 is the slot length, and parameters L2, d2 and x2 (the length, position and width of the downward vertical feed stubs), directly affect the amount of coupling between feed and slot, resulting in the change of the effective slot length and the resonant frequency.
- The return loss level is mainly determined by L2 and the patch length (B). Since L2 is the length of downward stubs, and the length of upward stubs is determined by the difference B-L2.
- The change of the parameters B, L2 and Ls2 can play an important role to put the two neighbouring resonances closer together, to form one broad bandwidth.

Table 2. Influence of the main parameters.

Parameter	f1	f2	fc	f2- f1	RL level
A+	-	--	-	-	+
B+	--	-	--	++	--
d2+	+	+	+	0	0(-)
H+	0	0(+)	+	0(+)	0(-)
L2+	+	--	+	--	--
Ls1+	+	0(+)	0	-	0
Ls2+	0(-)	--	-	--	+
w1+	0	0	0	0	0
w2+	0	0	0	0	0(-)
x1+	0(-)	0(-)	0	0	0(-)
x2+	0	+	0	+	-
x3+	0(-)	0	0	0(+)	0(-)
x4+	+	0(-)	0	-	+
x5+	-	0	0	+	-

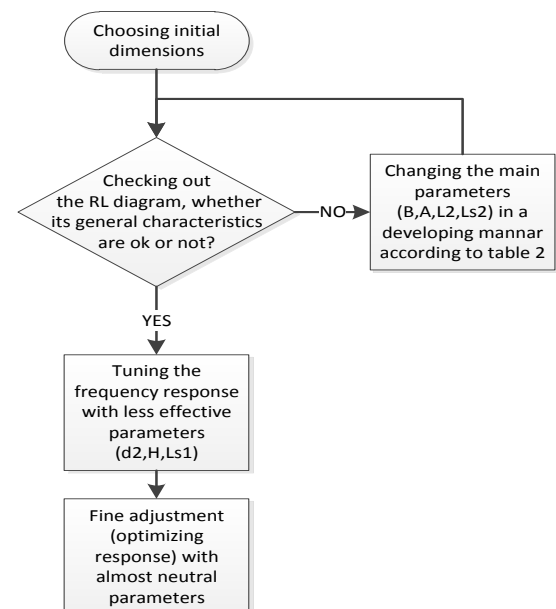


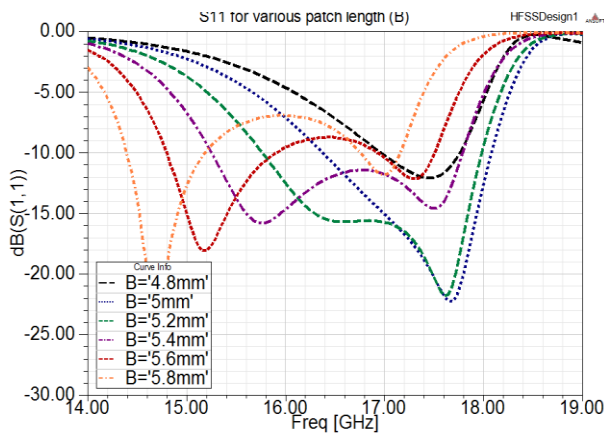
Figure 3. Design procedure flowchar

#### IV. DESIGN PROCEDURE

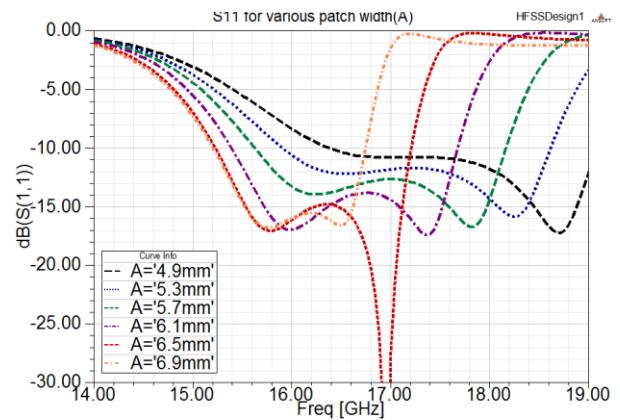
By recognizing the effect of each parameter, now some design guidelines are obtained. Considering the data in Table 2, a design procedure can be developed in the following steps:

First, the patch dimensions are obtained using the basic rules of designing a simple patch antenna [17] (the patch width is usually a little longer than the patch length, which is set to be a little less than half of the guided wavelength). In [18] some approximate relations are presented for resonant frequencies of a “probe-fed” U-slotted patch antenna in terms of the patch and U-slot arms dimensions. As a good starting point, these relations can be used to determine the initial values for the lengths of the U-slot arms. Finally, initial values of other parameters should be chosen regarding to the limitations such as the minimum practical width of microstrip lines. With these dimensions, an initial return loss is obtained. Then the main parameters, i.e., B, A, L2, Ls2 in a developing manner should be changed according to Table 2. **Figure 4(a)** depicts that how the patch

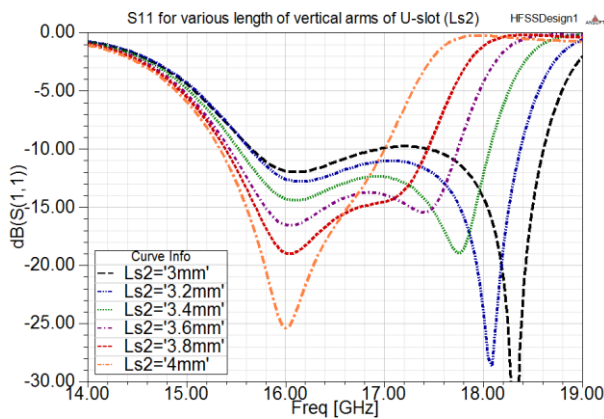
length (B) is the principal parameter to adjust the central frequency and to obtain an appropriate impedance matching. But, as it influences on all the parameters intensely, it would be better to be adjusted first, and not to be changed any more afterwards. **Figure 4 (b)** and (c), show that lengths A and Ls2, can be properly changed to vary the second resonant frequency. In **Figure 4(d)**, it is observed that L2 can be especially changed to increase the return loss level. This stage can be repeated until an almost acceptable response is obtained. Then, this response can be tuned with other parameters mentioned already as less effective ones (such as d2, H, Ls1). For improving one characteristic, it is preferred to change parameters which their influences on other characteristics are negligible. Finally, fine adjustment can be achieved by other almost neutral parameters until an optimum response is obtained. These steps are shown in Figure 3 as the design flowchart.



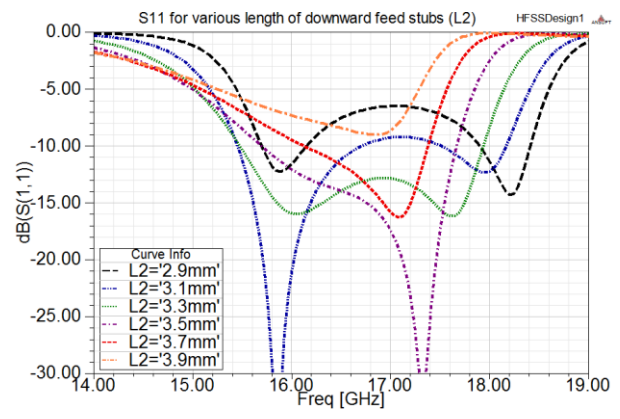
(a)



(b)



(c)



(d)

**Figure 4.** Influence of the main parameters in the reflection coefficient of the single-element antenna.

## V. THE DESIGN OF ANTENNAS AND RESULTS

A single-element antenna was designed at center frequency of 16.7 GHz according to the previous sections. Also,  $1 \times 2$  and  $2 \times 2$  uniform arrays of this element were designed. The results are presented as follows.

### A. Single element

After designing the antenna, a quarter-wavelength transformer is used to match the 74-ohms input impedance of the antenna to 50-ohms microstrip feed-line. The fabricated antenna, connected to a 50 ohms SMA, is shown in **Figure 5(a)**. The ground of the antenna structure is simply soldered to the SMA flange. It should be noted that the fabrication of multiple thin stubs and slots in the structure is so sensitive to the implementation tolerances. Meanwhile, embedding the SMA connector tab between the two layers may cause a tiny air gap there. Some possibilities for implementation method are compared in [19]. It is seen that the method of soldering the connector to the structure, effectively influences on the antenna return loss. Regarding these tolerances, a good agreement between simulation and measurement results of reflection coefficient is observed in Figure 6. The -

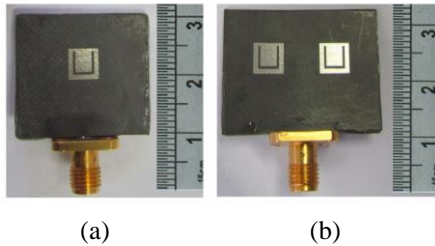


**Figure 5.** Photos of the fabricated antennas.

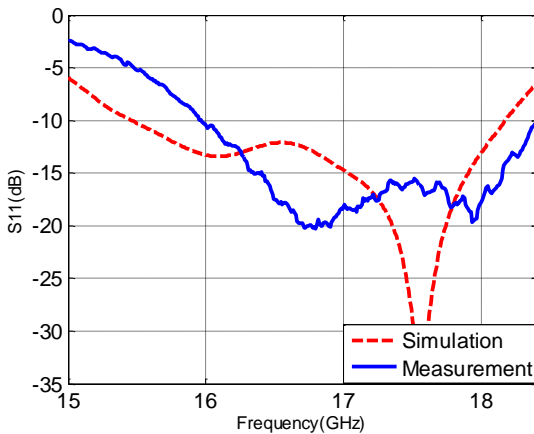


**Figure 6.** Reflection coefficient of the single-element antenna.

10dB impedance bandwidth, is 2.71GHz in the simulation and 2.45GHz in the measurement, which is about 15% for the center frequency of 16.7GHz. The simulation and measurement results of radiation patterns, for two frequencies are illustrated in Figure 7 to Figure 10. The H-plane pattern is symmetric; however, the E-plane pattern is expected to be asymmetric due to the feed-line in one side of the patch with U-slot. Since the antenna feeding was done through an SMA connector presented in the antenna E-plane, there is an additional disturbance in E-plane pattern in simulation due to the effect of SMA flange operating as a reflector with considerable size compared with the antenna. In addition, embedding the SMA tab between the two layers of the antenna causes an air gap, which mainly exists around the antenna feed entrance, and its destructive effect is more evident in the single-element-antenna measured E-plane pattern. This air gap between layers, as an imperfection in fabrication, causes the measured E-plane X-pol to be higher than the simulated X-pol level. The simulated and measured gains at 18 GHz are 8.6dB and 9.07dB, respectively, at the symmetry axis of the antenna.

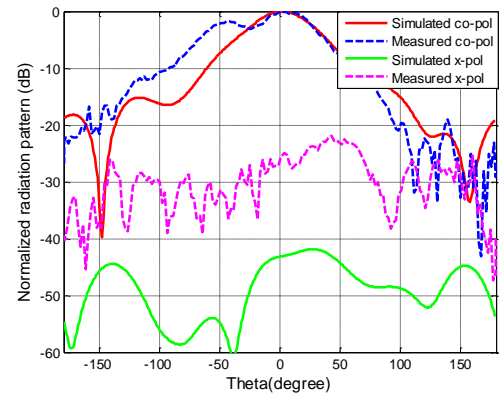


**Figure 7.** E-plane radiation pattern of the single element at 16.7GHz.

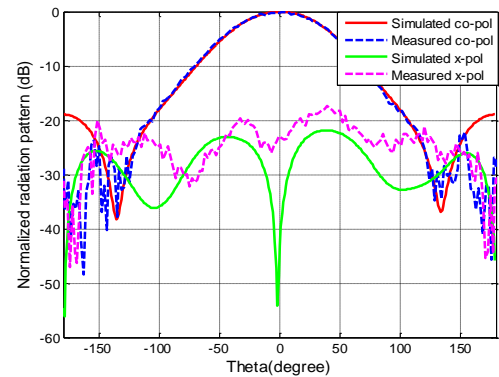


**Figure 8.** H-plane radiation pattern of the single element at 16.7GHz.



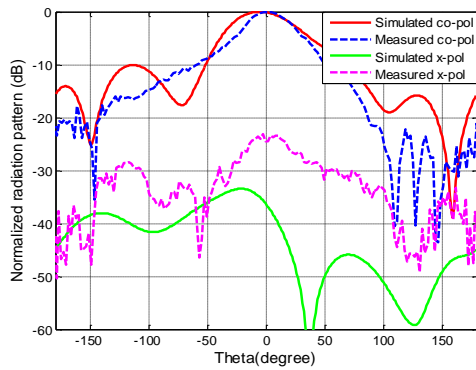


**Figure 9.** E-plane radiation pattern of the single element at 18GHz.

### B. Two-element array

The configuration of the  $1 \times 2$  array antenna is shown in Figure 11. The distance between elements is about one half of the wavelength of the substrate. In order to compensate the discontinuity effects at bends in the feed-lines, chamfered bends are used instead of the right-angled bends. Also, T-junction with a triangular notch as seen in Figure 11, in comparison with an ordinary T-junction results in a better return loss [20]. The length and angle of the triangular notch and chamfered bends are optimized. The simulated and measured

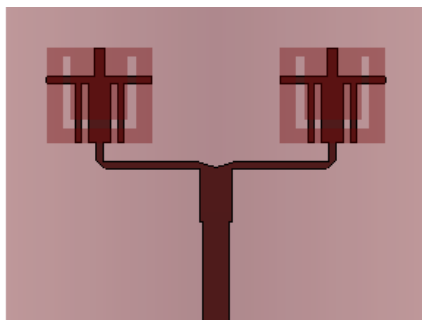


**Figure 11.** The top view of the  $1 \times 2$  array antenna.

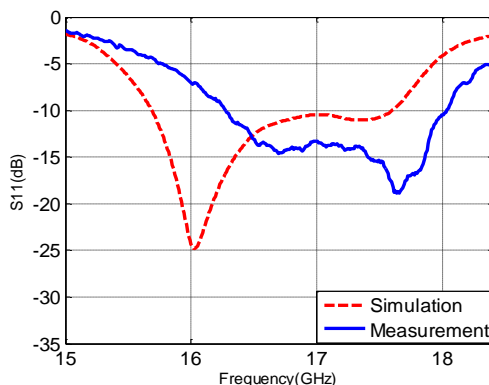


**Figure 12.** Reflection coefficient of the two-element array antenna.

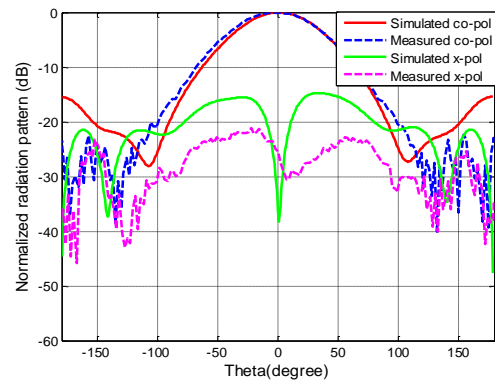


**Figure 10.** H-plane radiation pattern of the single element at 18GHz.

reflection coefficient diagrams of the array are depicted in Figure 12 which shows -10dB bandwidth of 1.91GHz and 1.77GHz in the simulation and measurement results, respectively. The radiation patterns for two frequencies are illustrated in Figure 13 to Figure 16. The asymmetry of the H-plane patterns may be due to the non-uniform undesirable gap between the layers during fabrication, and the elements which are not exactly the same. As seen in the figures, the radiation patterns are almost stable in the two frequencies within the bandwidth.

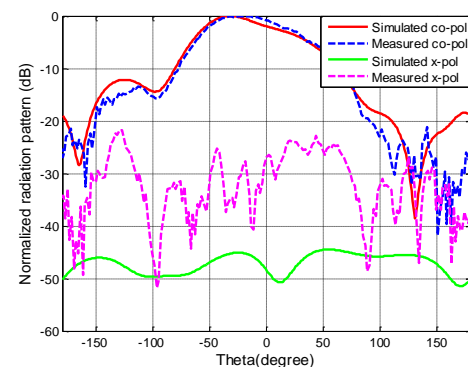


**Figure 13.** E-plane radiation pattern of the two-element array at 16.7GHz.

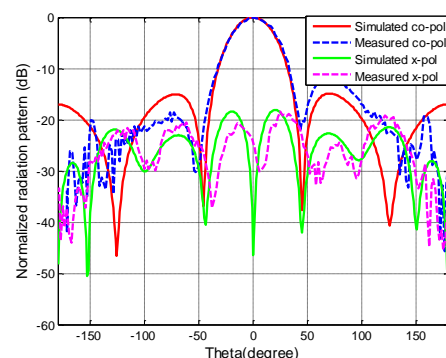


**Figure 14.** H-plane radiation pattern of the two-element array at 16.7GHz.

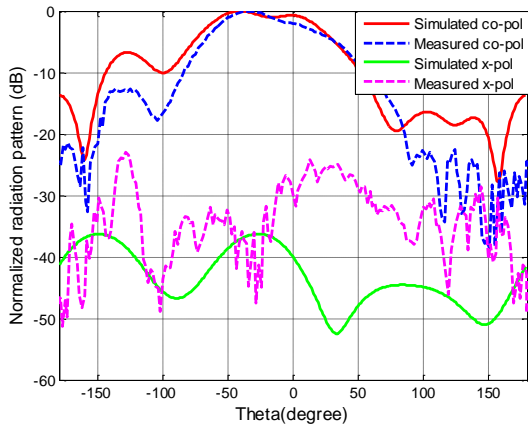


**Figure 15.** E-plane radiation pattern of the two-element array at 18GHz.

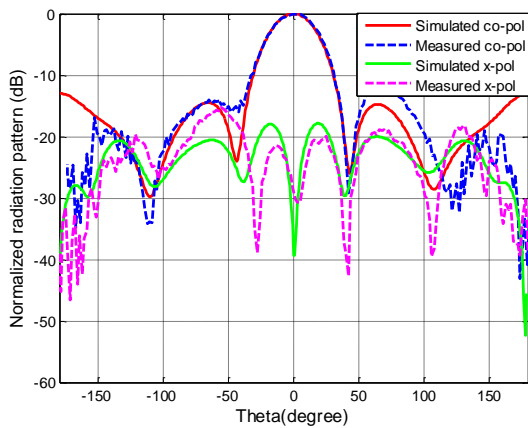


**Figure 16.** H-plane radiation pattern of the two-element array at 18GHz.

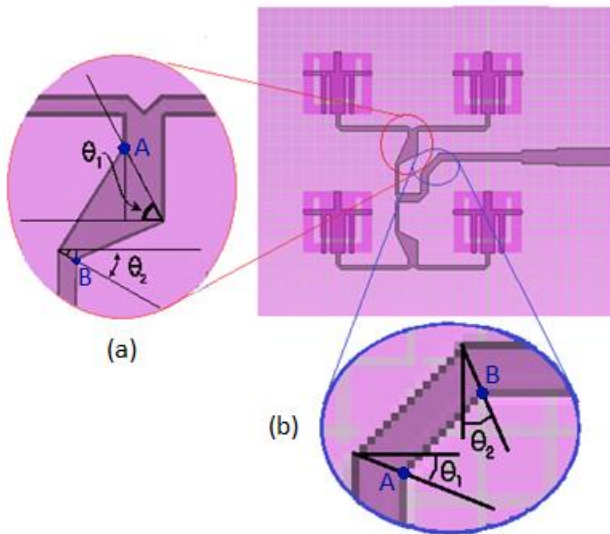


**Figure 17.** The top view of the 2x2 array antenna.

### C. 2x2 array

A four-element array, with uniform current distribution, is shown in Figure 17. Chamfered bends and T-junctions with triangular notches are used again. The feed network is designed to match the array antenna to 50 ohm microstrip line in such a way resulting in fewer discontinuities. However, practical constraints of fabrication restrict the minimum line width. Regarding to the finer details shown in blowup sections in Figure 17, a new connection for microstrip lines was proposed to act as a two-obtuse-angled bend. With tuning two slippery points (A and B), the discontinuity loss can be minimized by optimizing  $\theta_1$  and  $\theta_2$ . This kind of connection is applicable in connecting parallel microstrip lines (such as Figure 17(a)), as well as perpendicular ones (such as Figure 17(b)). Therefore, it provides more flexibility to choose the length of connected feed-lines. The resultant simulated and measured reflection coefficients of the antenna are in a good agreement as shown in Figure 18. The resultant -10dB bandwidth is 2.33GHz in simulation and 2.43GHz in measurement. Also the simulation results of radiation patterns are presented in Figure 19 to Figure 22. Regarding to the feed-line in the antenna H-plane, the pattern is no more symmetric, and X-pol radiation is increased in this plane, but this discrepancy is not observed in larger arrays with symmetric feed network.

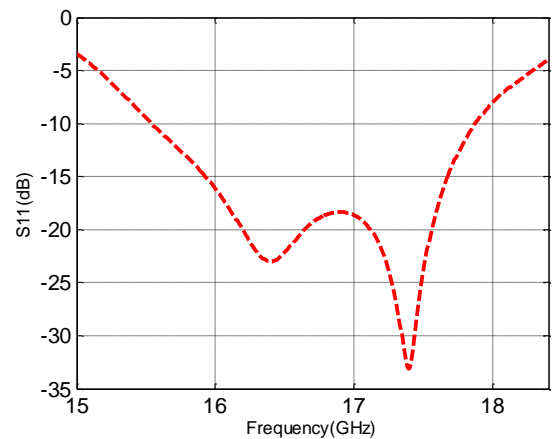


**Figure 18.** Reflection coefficient of the simulated 2x2 array antenna.

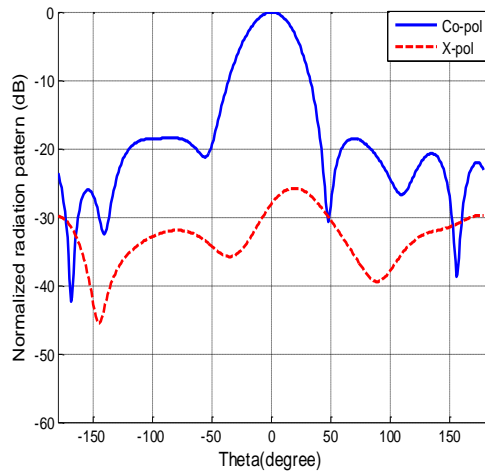


**Figure 19.** E-plane simulated radiation pattern of the  $2 \times 2$  array antenna at 16.7GHz.

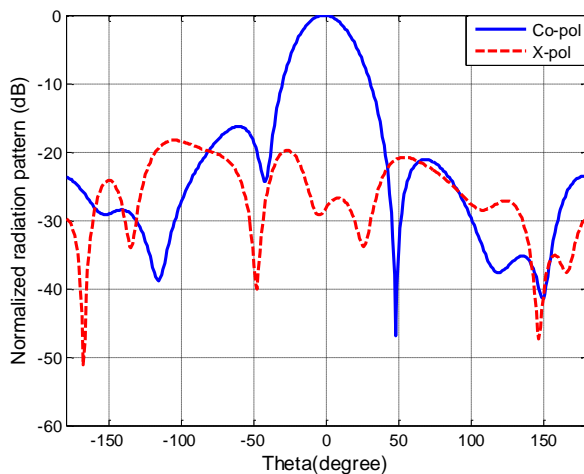


**Figure 20.** H-plane simulated radiation pattern of the  $2 \times 2$  array antenna at 16.7GHz.

## VI. CONCLUSION

This paper investigates and recognizes the main parameters to design a Ku-band proximity coupled-fed, U-slot microstrip antenna, based on the parametric studies. It also presents the effect of each parameter on the frequency response behavior of the antenna. Some steps were proposed to design a single-element antenna. The single antenna and  $1 \times 2$  and  $2 \times 2$  array antennas were designed and considered in which the feed networks were clearly described, and the simulation and measurement results of single antenna and  $1 \times 2$  array antenna were compared.

## ACKNOWLEDGMENT

The authors would like to thank ICTI (Information and Communication Technology Institute) for supporting this project.

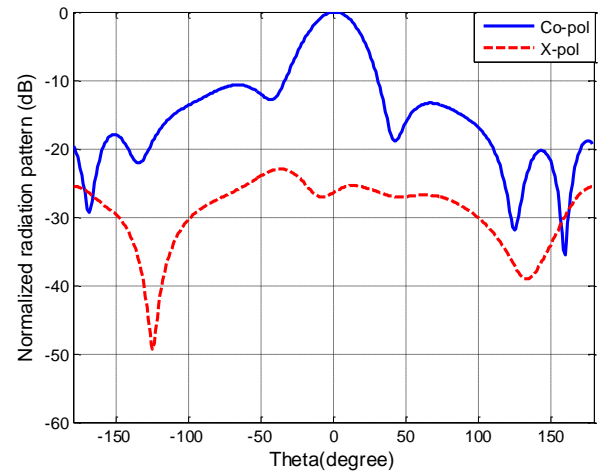


**Figure 21.** E-plane simulated radiation pattern of the  $2 \times 2$  array antenna at 18GHz.

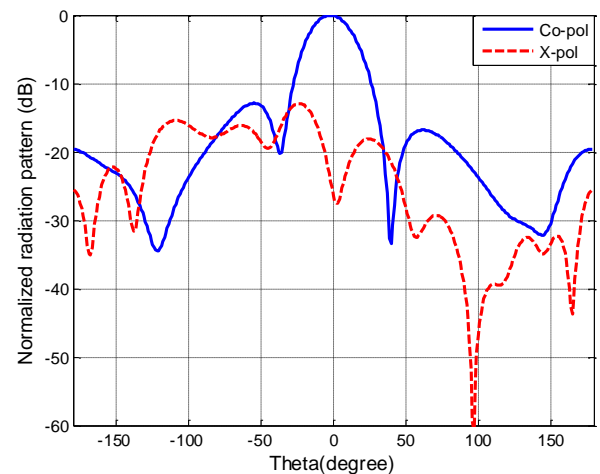


**Figure 22.** H-plane simulated radiation pattern of the  $2 \times 2$  array antenna at 18GHz.

## REFERENCES

- [1] D. M. Pozar, *The Analysis and Design of Microstrip Antennas and Arrays*. Wiley interscience, 1995.
- [2] S. Bhunia, "Effects of slot loading on microstrip patch antennas" *International Journal of Wired and Wireless Communications*, vol.1, no. 1, 2012.
- [3] T. Huynh and K. Lee, "Single-layer single-patch wideband microstrip antenna" *Electronics Letters*, vol. 31, no. 16, 1995, pp. 1310-1312.
- [4] K. Lee, S. Steven Yang, A. Kishk and K. Luk, "The versatile U-slot patch antenna" *IEEE Antennas Propag. Mag.*, vol. 52, no. 1, 2010, pp. 71-88.
- [5] C. Mak, K. Luk and K. Lee, "Proximity-coupled U-slot patch antenna" *Electron. Lett.*, vol. 34, no. 8, 1998, p. 715.
- [6] B. Ooi, "A double-II stub proximity feed U-slot patch antenna" *IEEE Transactions on Antennas*



- and Propagation, vol. 52, no. 9, 2004, pp. 2491-2496.
- [7] C. Kidder, Ming-yi Li and Kai Chang, "Broadband U-slot patch antenna with a proximity-coupled double  $\Pi$  -shaped feed line for arrays" IEEE Antennas and Wireless Propagation Letters, vol. 1, no. 1, 2002, pp. 2-4.
- [8] B. Strassner, "Lightweight, wideband, amplitude-tapered, linearly-polarized, dual-axis monopulse, Ku-band patch antenna array for SAR" IEEE Antennas and Propagation Society International Symposium, 2007.
- [9] K. Lee, K. Luk, K. Tong, S. Shum, T. Huynh and R. Lee, "Experimental and simulation studies of the coaxially fed U-slot rectangular patch antenna" IEE Proceedings - Microwaves, Antennas and Propagation, vol. 144, no. 5, 1997, p. 354.
- [10] Chow, Y.L., Chen, Z.N., Lee, K.F. and Luk, K.M., "A design theory on broadband patch antennas with slot" IEEE Antennas and Propagation Society International Symposium, 1998, pp. 1124 - 1127.
- [11] J. Ansari and R. Brij Ram, "Analysis of broad band U-slot microstrip patch antenna" Microwave and Optical Technology Letters, vol. 50, no. 4, 2008, pp. 1069-1073.
- [12] S. Weigand, G. Huff, K. Pan and J. Bernhard, "Analysis and design of broad-band single-layer rectangular u-slot microstrip patch antennas" IEEE Transactions on Antennas and Propagation, vol. 51, no. 3, 2003, pp. 457-468.
- [13] R. Bhalla and L. Shafai, "Resonance behavior of single U-slot microstrip patch antenna" Microwave and Optical Technology Letters, vol. 32, no. 5, 2002, pp. 333-335.
- [14] J. Jacobs, "Efficient resonant frequency modeling for dual-band microstrip antennas by gaussian process regression" IEEE Antennas and Wireless Propagation Letters, vol. 14, 2015, pp. 337-341.
- [15] R. Garg, P. Bhartia, I. Bahl and A. Ittipiboon, Microstrip Antenna Design Handbook. Artech House INC., 2001.
- [16] Z. N. Chen, M. Y. W. Chia, Broadband planar antennas. Wiley publication, 2006.
- [17] C. A. Balanis, Modern Antenna Handbook. John Wiley & Sons INC., 2008.
- [18] R. Shafai and L. Bhalla, "Resonance Behavior of Single U-Slot Microstrip Patch Antenna", Microwave and Optical Technology Letters, Vol.32, No.5, pp. 333–335, 2002.
- [19] M. Nasirian, M. Maddah-Ali, Z.H. Firouzeh and Gh. Askari, "The effect of SMA connector implementation on a two-layer Ku-band microstrip antenna" The third Iranian Conference on Engineering Electromagnetic (ICEEM), 2014.
- [20] K.C. Garg, R. Bahl, I. Bhartia, and P. Gupta, Microstrip lines and slotlines. Artech House Microwave Library, 1996.